Journal of The Electrochemical Society, **157** (3) B365-B369 (2010)
0013-4651/2010/157(3)/B365/5/$28.00 © The Electrochemical Society

A Comparison of Molten Sn and Bi for Solid Oxide Fuel Cell Anodes

A. Jayakumar,[a] S. Lee,[a] A. Hornés,[b] J. M. Vohs,[a,*] and R. J. Gorte[a,*,z]

[a]*Department of Chemical and Biomolecular Engineering, University of Pennsylvania, Philadelphia, Pennsylvania 19104, USA*
[b]*Institute of Catalysis and Petrochemistry, Consejo Superior de Investigaciones Científicas, 28049 Madrid, Spain*

Molten Sn and Bi were examined at 973 and 1073 K for use as anodes in solid oxide fuel cells with yttria-stabilized zirconia (YSZ) electrolytes. Cells were operated under "battery" conditions, with dry He flow in the anode compartment, to characterize the electrochemical oxidation of the metals at the YSZ interface. For both metals, the open-circuit voltages (OCVs) were close to that expected based on their oxidation thermodynamics, ~0.93 V for Sn and ~0.48 V for Bi. With Sn, the cell performance degraded rapidly after the transfer of approximately 0.5–1.5 C/cm^2 of charge due to the formation of a SnO_2 layer at the YSZ interface. At 973 K, the anode impedance at OCV for freshly reduced Sn was approximately 3 Ω cm^2 but this increased to well over 250 Ω cm^2 after the transfer of 1.6 C/cm^2 of charge. Following the transfer of 8.2 C/cm^2 at 1073 K, the formation of a 10 μm thick SnO_2 layer was confirmed by scanning electron microscopy. With Bi, the OCV anode impedance at 973 K was less than 0.25 Ω cm^2 and remained constant until essentially all of the Bi had been oxidized to Bi_2O_3. Some implications of these results for direct carbon fuel cells are discussed.
 [DOI: 10.1149/1.3282443]

Manuscript submitted September 21, 2009; revised manuscript received November 30, 2009. Published January 19, 2010.

It is theoretically possible to convert solid carbonaceous fuels, including biomass or coal, directly into electricity using fuel cells based on electrolytes that transfer oxygen ions.[1-9] A major challenge in making these direct carbon fuel cells (DCFCs) practical is the requirement of fabricating low impedance anodes that allow facile transfer of oxygen from the electrolyte to the surface of the solid fuel. Although this transfer can be accomplished in the gas phase using a CO–CO_2 redox couple,[3] the use of electrodes based on liquid metals and molten carbonates would offer improved fuel flexibility.[4-9]

The majority of work in DCFC has used a mixture of molten-carbonate salts (e.g., $Li_2CO_3 + K_2CO_3 + Na_2CO_3$) as the anode, using either a molten-carbonate or a yttria-stabilized zirconia (YSZ) electrolyte.[10] Although the mixed carbonate salts appear to be very good oxidizers and impressive performance levels have been achieved with this type of anode, molten carbonates are not electronically conductive so that a metallic current collector must be incorporated into the anode structure. In addition to the problems associated with dissolution of metals like Ni into the salt solution, the anode half-cell reaction, Reaction 1, requires transfer of electrons so that only the fuel, which is in contact with the current collector, can be oxidized

$$C + 2O^{2-} = CO_2 + 4e^- \quad [1]$$

The situation is completely analogous to what happens in normal solid oxide fuel cell (SOFC) electrodes, where reaction can only occur at three-phase boundary sites, that line where the gas phase, the electronic conductor, and the ionic conductor all come together.[11] One method for increasing the region where Reaction 1 can occur involves using a conductive form of carbon as the fuel and maintaining a high concentration of that carbon within the carbonate solution.[2] This obviously limits what fuels can be used because the fuel itself is part of the anode.

Another approach for transferring oxygen from the electrolyte to the solid fuel involves the use of anodes composed of liquid metals, such as Sn or Bi.[8-10,12] In this case, the metal reacts at the electrolyte interface via Reaction 2, and the metal oxide (MO) is in turn reduced by the carbonaceous fuel in a separate step

$$M + nO^{2-} = MO_n + 2ne^- \quad [2]$$

For cells using Sn anodes, it has been reported that this type of fuel cell can be operated in a "battery" mode by simply allowing the metallic Sn to be consumed and then be regenerated later.[9] However, while the concept has been demonstrated with liquid Sn anodes, there is very little fundamental information available to show what limits the performance of these electrodes and how one might improve them.

In the present paper, we set out to investigate Reaction 2 in a fuel cell with a YSZ electrolyte, using Sn or Bi as the anode. With Sn, we show that a critical issue that limits performance at temperatures below 1073 K is the formation of a SnO_2 film at the electrolyte interface due to the very low solubility of oxygen in molten Sn.[13] The performance of the Sn-based electrodes appears to be limited by the low ionic conductance of this SnO_2 layer, at least for temperatures below 1073 K. With molten Bi, the electrochemical reaction is facile, probably because the oxide is a good ionic conductor;[14] however, the critical issue with Bi is its lower open-circuit potential.

Experimental

The electrolyte and cathode of the fuel cells used in this study were prepared in a manner similar to that described in previous work from our laboratory.[15-18] First, a YSZ wafer, with one side porous and one side dense, was produced by laminating two green tapes, using graphite as the pore former in the layer that was to be porous, and then firing the structure to 1773 K for 4 h. The dense electrolyte layers were approximately 900 μm thick while the porous layers were 50 μm thick. Both the dense and the porous layers were circular, but the diameter of the dense layers was 1 cm and the diameter of the porous layers was 0.67 cm. To produce 40 wt % $La_{0.8}Sr_{0.2}FeO_3$–YSZ (LSF–YSZ) composite cathodes, the porous layers were impregnated with an aqueous solution of $La(NO_3)_3$, $Fe(NO_3)_3$, and $Sr(NO_3)_2$ in the proper molar ratios, followed by calcination to 1123 K.[16,17]

After preparation of the cathode, the cell was mounted onto an alumina tube using a ceramic adhesive (Aremco Ceramabond 522). The tube was then mounted vertically so the molten metal could be kept in contact with the YSZ electrolyte by gravity. A ceramic bar of either $La_{0.3}Sr_{0.7}TiO_3$ (LST) or $La_{0.8}Sr_{0.2}CrO_3$ (LSCr) was suspended in the molten metal above the electrolyte for current collection. In initial studies with Sn, the ohmic impedances of the cells were much greater than that expected based on the electrolyte thickness because the molten Sn did not "wet" the YSZ electrolyte, forming instead spheres that made poor contact with the YSZ surface. To solve this

* Electrochemical Society Active Member.
z E-mail: gorte@seas.upenn.edu

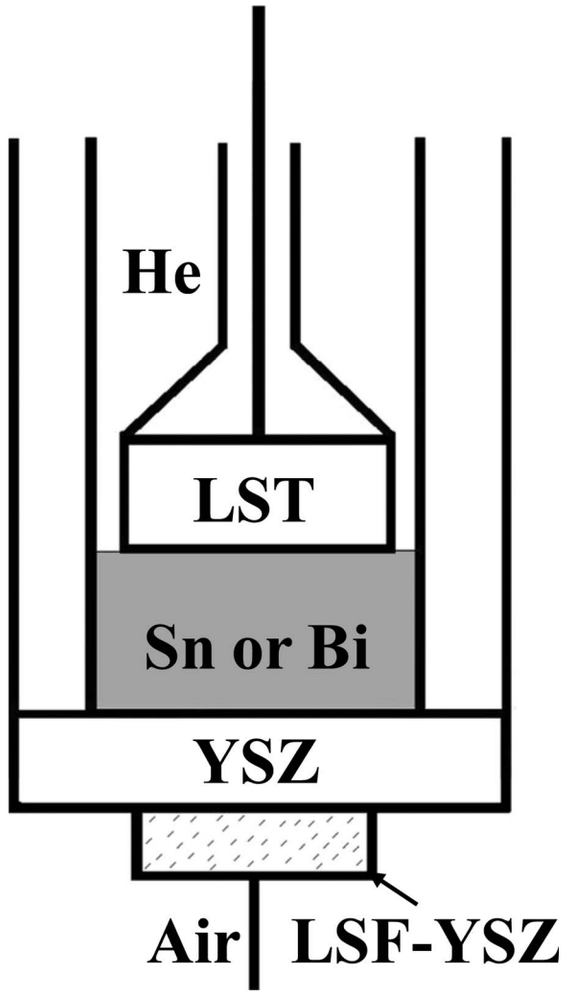

Figure 1. Schematic of the experimental system.

problem, the ceramic current collector was made into a circular wafer and attached to an alumina tube that allowed the metal to be "pressed" onto the electrolyte, as shown in Fig. 1. Notice that the porous separator in other work with Sn anodes likely plays a similar role in maintaining contact between Sn and the electrolyte.[8] Ag wire was passed through the alumina tube for electrical contact with the ceramic current collector. For the present study, 800 mg of either Sn (Aldrich) or Bi (Aldrich) was added to the anode compartment. Based on the density of metals and the inner diameter of the tube used for the anode compartment, this resulted in metal layers that were approximately 1.5 mm thick.

For electrochemical characterization, the cathode was held in air and a gas flow was maintained over the anode. Because we were interested in Reaction 2, most experiments were conducted in the battery mode. The anodes were first reduced in humidified (3% H_2O) H_2, but the electrochemical measurements were performed while flowing dry He into the anode compartment. Impedance spectra and voltage–current (*V-i*) polarization curves were measured using a Gamry Instruments potentiostat. Impedance spectra were measured galvanostatically at various currents in the frequency range of 300 kHz–0.1 Hz, with a 1 mA ac perturbation. We used the average of the anode and cathode diameters to calculate the effective electrode area, which was then used to normalize the current densities. Because the ionic conductivity of YSZ is well known[18] and the impedance of the infiltrated LSF-YSZ cathode has been extensively

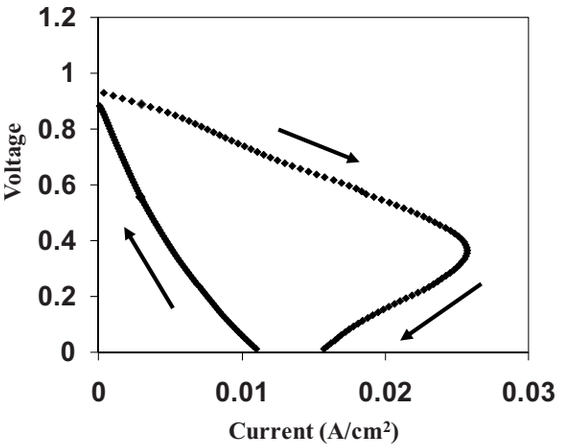

Figure 2. *V-i* polarization curve for the cell with the molten Sn anode at 973 K. After reduction of the Sn in humidified H_2, the anode compartment was exposed to dry, flowing He while ramping the voltage from open circuit and back at 10 mV/s.

characterized in previous studies,[14,15] the performance of the molten-metal anodes could be determined by difference.[12]

Scanning electron microscopy (SEM) was performed using a JEOL 7500F HRSEM, together with energy-dispersive X-ray spectroscopy (EDX).

Results

Molten Sn anodes.— Figure 2 shows the *V-i* characteristics of the cell with the molten Sn anode at 973 K. In this experiment, the anode compartment was reduced in flowing, humidified (3% H_2O) H_2 while holding the cell at open circuit. After flushing the H_2 from the anode compartment with dry He, the initial open-circuit voltage (OCV) of the freshly reduced cell was approximately 0.93 V, very close to the expected potential for the oxidation of Sn, Reaction 3, when referenced to air[12]

$$Sn + 2O^{2-} = SnO_2 + 4e^- \quad [3]$$

Next, the current generated by the cell was measured while decreasing the potential at 10 mV/s. After the cell potential reached zero, the potential was ramped up at 10 mV/s. The data show that the current reached a maximum as the potential was lowered and then began to decrease. The decrease in current was not reversed by increasing the potential. Results obtained at 1073 K were qualitatively similar to those shown in Fig. 2.

The impedance measurements in Fig. 3 demonstrate that the changes occurring in the cell are associated with the anode. Figure 3a is the Cole–Cole plot of the reduced cell at 973 K in dry He before applying any current. The high frequency intercept with the real axis, which corresponds to the ohmic resistance of the cell, occurs at 5.37 Ω cm^2 and is reasonably close to the expected value of 4.7 Ω cm^2 for the measured YSZ electrolyte thickness of this cell, 890 μm, based on tabulated conductivity of YSZ at 973 K, 0.0188 S/cm.[18] The nonohmic impedance, determined from the difference between the low and high frequency intercepts, is approximately 3 Ω cm^2. Because the contribution from the LSF-YSZ cathode at this temperature is between 0.1 and 0.2 Ω cm^2,[16,17] most of the nonohmic contribution is from the Sn anode. Figure 3b shows the impedance data at OCV after completing a cycle like that shown in Fig. 2. The ohmic resistance has not changed significantly, demonstrating that the electrode retains high electronic conductivity. However, the nonohmic losses in the cell are now enormous, approximately 250 Ω cm^2. Experiments performed at 1073 K gave results that were qualitatively similar.

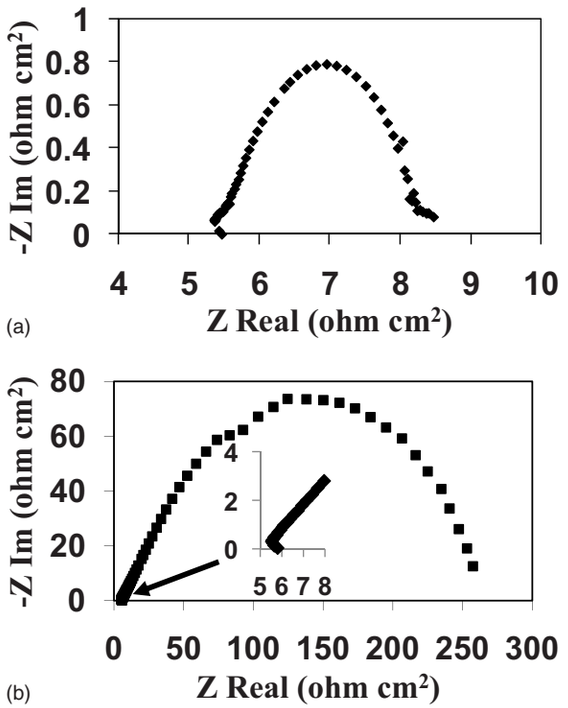

Figure 3. Impedance data for the cell with the molten Sn anode at 973 K, corresponding to the *V-i* polarization data in Fig. 2. (a) Cole–Cole plot obtained near the open circuit immediately after reduction of the Sn. (b) Cole–Cole plot after completing the ramp from the open circuit to 0 V and back.

The drop in current and increase in impedance are related to the amount of charge that had been drawn from the cell. When experiments like that shown in Fig. 2 were conducted at lower ramp rates, the maximum current occurred at lower values. Measurements at 1073 K with ramp rates between 1 and 10 mV/s indicated that the total amount of charge transferred across the electrolyte was nearly constant, between 4 and 6 C/cm^2, before the impedance became very large. Furthermore, once this charge had been transferred, the only way to restore the low impedance of the cell was to expose the anode to flowing H_2 for at least 30 min. Holding the cell at OCV in flowing He overnight had no effect on the impedance. These results suggest that the increased impedance is due to the formation of a dense SnO_2 layer at the electrolyte interface. Once this layer is formed, oxidation of additional Sn is limited by transport of oxygen through the SnO_2 layer and the low solubility of oxygen in liquid Sn, which is only 0.10 mol % at 1073 K.[13]

To confirm that cell deactivation was due to the formation of an oxide layer at the YSZ interface, we performed a *V-i* cycle like that shown in Fig. 2 at 1073 K, then cooled the cell to room temperature, broke the cell, and examined the YSZ interface using SEM and EDX. The total charge transferred in this experiment was 8.2 C/cm^2, which corresponds to the formation of a SnO_2 layer that is 4.6 μm thick. As shown in Fig. 4, this oxide layer is readily apparent in the cross-sectional SEM image. The SEM and EDX data indicate that there is indeed a SnO_2 layer, approximately 10 μm thick, at the YSZ interface. The somewhat larger SEM thickness is likely due to the SnO_2 layer being somewhat porous. Also, EDX results indicated that some SnO_2 on spherical particles was farther from the electrolyte interface. It is unclear if this results from the process of fracturing the Sn-YSZ interface or if this is an indication that some SnO_2 may extend some distance from the YSZ electrolyte interface.

Molten Bi anodes.— Bi has a similar melting temperature to that of Sn (545 K vs 505 K) so that it was of interest to examine the

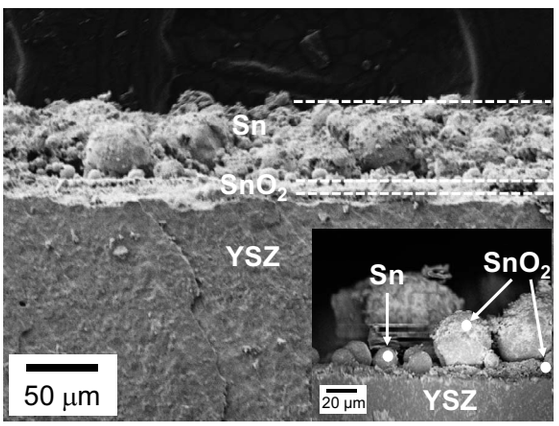

Figure 4. SEM and EDX results obtained at the molten Sn/YSZ electrolyte interface. The micrograph was obtained after passing 8.2 C/cm^2 of charge through the electrolyte at 1073 K, then quenching to room temperature, and shows the formation of a SnO_2 layer at the YSZ interface.

characteristics of a cell with a molten Bi anode. We again operated the cell in a battery mode, with dry He flowing into the anode compartment after reducing the Bi, so that the electrochemical oxidation of the metal, Reaction 4, could be studied

$$Bi + 1.5O^{2-} = BiO_{1.5} + 3e^- \quad [4]$$

The mass of Bi used in the anode was also 800 mg, the same as that used for the Sn anode. The *V-i* plot at 973 K in Fig. 5 shows many important differences from that observed for the cell with the Sn anode. First, in agreement with expectations based on the thermodynamics of Reaction 4, the OCV is only 0.48 V. Second, the *V-i* polarization plot is a straight line that exhibited complete reversibility when the potential was ramped up or down.

The Cole–Cole plot for the Bi cell, shown in Fig. 6, demonstrates that the impedance of the Bi anode was very small. The ohmic impedance was again 4.8 Ω cm^2, close to the value of 5.27 Ω cm^2 expected for the 990 μm YSZ electrolyte. However, unlike the case for the cell with the Sn anode, the nonohmic impedance for the cell with the Bi anode was very low, only 0.22 Ω cm^2. Because this is close to the impedance of the LSF-YSZ cathode,[16,17] the anode losses must be negligible. The fact that the *V-i* plot in Fig. 5 was linear implies that impedance remains low under applied currents.

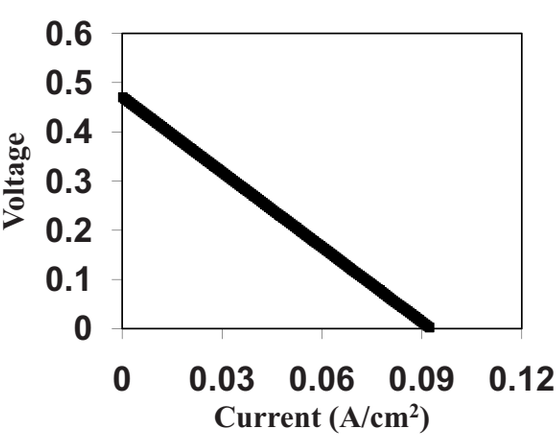

Figure 5. *V-i* polarization curve for the cell with the molten Bi anode at 973 K. After reduction of the Bi in humidified H_2, the anode compartment was exposed to dry, flowing He.

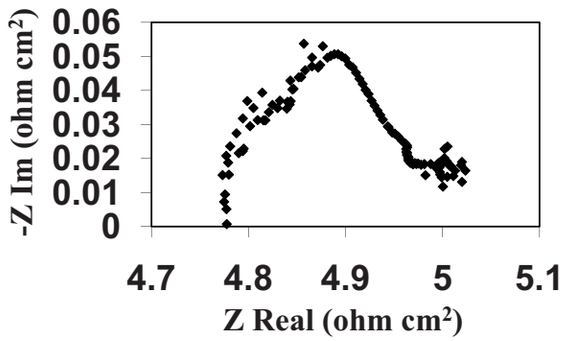

Figure 6. Impedance data for the cell with the molten Bi anode at 973 K, corresponding to the data in Fig. 5.

To determine how much of the metallic Bi was accessible for oxidation in the cell, we measured the cell potential at a constant current density of 40 mA/cm^2 as a function of time at 973 K, with the results shown in Fig. 7. Literature data indicate that the solubility of oxygen in molten Bi at 973 K is very low, 0.38 mol %,[19] so that deactivation processes similar to that observed with Sn are possible. However, Fig. 7 shows that the cell potential remained nearly constant for 13 h before dropping. Based on the charge that passed through the electrolyte during this time, approximately 85% of the metallic Bi reacted to Bi_2O_3 before significant changes were observed in the cell performance. Because the melting temperature of Bi_2O_3 is 1090 K, solid deposits must form at the YSZ interface with the Bi, just like those that formed with Sn. We suggest that the large difference between Bi and Sn is because Bi_2O_3 is a good ionic conductor,[14] allowing facile transfer of oxygen ions from the electrolyte to the metallic Bi.

Discussion

The comparison of Sn and Bi anodes for SOFC highlights the major requirements of liquid-metal anodes. First, one would like to have oxidation thermodynamics that result in a high OCV, similar to what is observed with Sn.[12] Second, there must be facile transfer of oxygen ions from the electrolyte to the metal. There may be multiple ways to deal with each of these issues.

Regarding the cell operating potential, the OCV is obviously regulated by the thermodynamics of the metal oxidation reaction when the cell is operated in a battery mode; however, the chemical potential of oxygen could be much lower in the molten metal when fuel is present. In this case, the theoretical OCV would be determined by the thermodynamics of the fuel oxidation reaction. This is obviously the situation for normal SOFC operation. For the Ni-based anodes that are commonly used in SOFC, great care is taken to avoid reaching the point at which Ni is in equilibrium with NiO. With metals like Bi and Sn, the question is whether the metals and their oxides are sufficiently catalytic to allow rapid oxidation of fuels that are dissolved within the anode. If the rate of fuel oxidation is rapid compared to the rate of oxygen transfer through the electrolyte, the cell potential is established by the fuel. Indeed, published *V-i* polarization curves for cells with liquid Sn anodes in the presence of flowing H_2 show OCV above 1 V,[8] implying that the OCV was established by H_2 oxidation, not by Reaction 3. While Bi and Sn are not exceptional oxidation catalysts, their tendency to form molten alloys with well-known catalytic metals, such as Ni, may allow improvements in the catalytic activity.

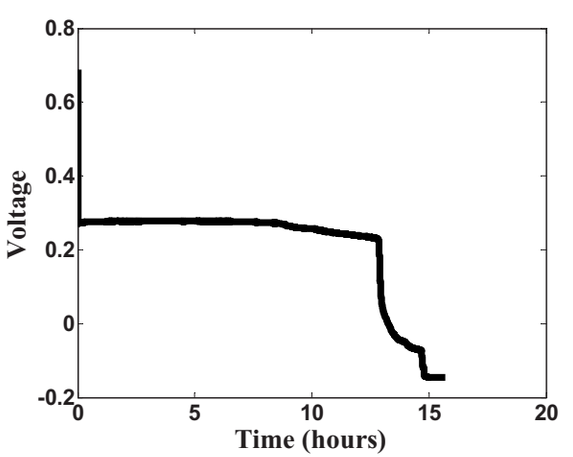

Figure 7. Cell voltage as a function of time for the cell with the molten Bi anode for a current of 40 mA/cm^2. The temperature was 973 K and a flow of dry He was maintained over the anode during the measurement.

While the facile oxygen transfer that we observed between YSZ and Bi is very encouraging, the deactivation observed following the formation of a dense SnO_2 layer at the YSZ interface needs to be avoided. Certainly, the effect of forming SnO_2 is much less at higher temperatures due to the higher solubility of oxygen in the molten Sn and due to higher ion diffusivity in the SnO_2, as demonstrated by the successful use of liquid Sn anodes in earlier work performed at 1273 K.[8,9] However, because the rate of all processes increases at the higher temperatures, the rate-limiting step at 1273 K likely remains diffusion of ions through SnO_2. The results of this study suggest two alternative paths for avoiding this problem. Using an M/MO_x system where the oxide has oxygen ion conductivity that is sufficiently high so that oxygen migration through the oxide does not limit performance is one approach. This is likely to be the case for Bi/Bi_2O_3. The second approach to limit the effect of oxide barriers is to work above the melting temperature of the oxides that form at the electrolyte interface. This could be difficult for metals like Sn because SnO_2 has a melting temperature of 1400 K, but relatively easy for Bi, because Bi_2O_3 melts at 1090 K. With mixed metals, it may also be possible to form lower melting temperature eutectics.

In any case, the molten-metal anodes appear to show significant promise. This remains an area that has not yet been extensively explored.

Conclusions

Two important factors have been identified as affecting the performance of molten-metal anodes for SOFC: the thermodynamic oxidation potential of the metal and the tendency for the oxide to form a film at the electrolyte interface. For operation of cells in the battery mode, where the metal is oxidized, the oxidation potential determines the OCV that can be achieved. Oxide films at the YSZ interface can effectively block charge transfer at the electrolyte interface if the oxide is a poor ionic conductor. However, both of these limitations have possible solutions, although further work is required to pursue these solutions.

Acknowledgments

This work was funded by the U.S. Department of Energy's Hydrogen Fuel Initiative (grant DE-FG02-05ER15721). A. J. was supported as part of the Catalysis Center for Energy Innovation, an Energy Frontier Research Center funded by the U.S. Department of Energy, Office of Science, Office of Basic Energy Sciences under award no. DE-SC0001004. A.H. thanks the MEC (Spain) for the FPU contract and also the Comunidad de Madrid (Spain), project ENERCAM S-0505/ENE/000304, for financial support.

University of Pennsylvania assisted in meeting the publication costs of this article.

References

1. D. Cao, Y. Sun, and G. Wang, *J. Power Sources*, **167**, 250 (2007).
2. B. Heydorn and S. Crouch-Baker, *Direct Carbon Conversion: Progressions of Power*, IOP, New York (2006).

3. S. Li, A. C. Lee, R. E. Mitchell, and T. M. Gür, *Solid State Ionics*, **172**, 1549 (2008).
4. K. Pointon, B. Lakeman, J. Irvine, J. Bradley, and S. Jain, *J. Power Sources*, **162**, 750 (2006).
5. Y. Nabae, K. D. Pointon, and J. T. S. Irvine, *Energy Environ. Sci.*, **1**, 148 (2008).
6. S. L. Jain, B. Lakeman, K. D. Pointon, and J. T. S. Irvine, *Ionics*, **13**, 413 (2007).
7. Y. Nabae, K. D. Pointon, and J. T. S. Irvine, *J. Electrochem. Soc.*, **156**, B716 (2009).
8. T. Tao, L. Bateman, J. Bentley, and M. Slaney, *ECS Trans.*, **5**(1), 463 (2007).
9. T. Tao, M. Slaney, L. Bateman, and J. Bentley, *ECS Trans.*, **7**(1), 1389 (2007).
10. Electric Power Research report no. 1016170, EPRI, Alto, CA (2008).
11. J. M. Vohs and R. J. Gorte, *Adv. Mater. (Weinheim, Ger.)*, **21**, 943 (2009).
12. T. Tao, in *Solid Oxide Fuel Cells IX (SOFC IX), Volume 1 Cells, Stacks, and Systems*, S. C. Singhal and J. Mizusaki, Editors, PV 2005-07, p. 353, The Electrochemical Society Proceedings Series, Pennington, NJ (2005).
13. T. A. Ramanarayanan and R. A. Rapp, *Metall. Trans.*, **3**, 3239 (1972).
14. D. J. L. Brett, A. Atkinson, N. P. Brandon, and S. J. Skinner, *Chem. Soc. Rev.*, **37**, 1568 (2008).
15. S. Park, R. J. Gorte, and J. M. Vohs, *J. Electrochem. Soc.*, **148**, A443 (2001).
16. Y. Huang, J. M. Vohs, and R. J. Gorte, *J. Electrochem. Soc.*, **151**, A646 (2004).
17. W. Wang, M. D. Gross, J. M. Vohs, and R. J. Gorte, *J. Electrochem. Soc.*, **154**, B439 (2007).
18. K. Sasaki and J. Maier, *Solid State Ionics*, **134**, 303 (2000).
19. D. Risold, B. Hallstedt, L. J. Gauckler, H. L. Lukas, and S. G. Fries, *J. Phase Equilib.*, **16**, 223 (1995).